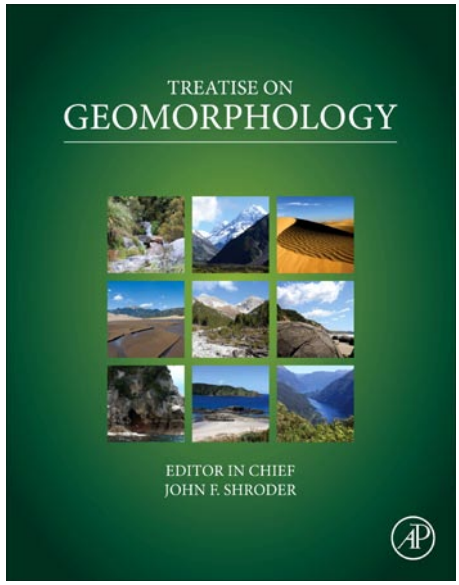

Heimsath A.M., and Jungers M.C. Processes, Transport, Deposition, and Landforms: Quantifying Creep. In: John F. Shroder (Editor-in-chief), Marston, R.A., and Stoffel, M. (Volume Editors). Treatise on Geomorphology, Vol 7, Mountain and Hillslope Geomorphology, San Diego: Academic Press; 2013. p. 138-151.

7.13 Processes, Transport, Deposition, and Landforms: Quantifying Creep

AM Heimsath and MC Jungers, Arizona State University, Tempe, AZ, USA

Glossary

Bioturbation The process of soil mixing driven by any biotic process.

Creep The process of downslope soil movement driven by a range of processes.

Freeze–thaw The process of soil mixing and downslope transport driven by the expansion and contraction caused by freezing and thawing of the soil.

Linear transport When soil flux is linearly proportional to hillslope gradient.

Nonlinear transport When soil flux is proportional to a function of hillslope gradient divided by a threshold gradient term.

Shrink–swell The process of soil mixing and downslope transport driven by expansion and contraction caused by the wetting and drying of the soil.

Abstract

Hilly upland landscapes are cloaked in a thin layer of soil derived primarily from the underlying parent material and transported by diverse processes. Creep subsumes soil transport processes assumed to be linearly proportional to slope and the authors examined a range of studies that have attempted to quantify these processes. This chapter thus provides a short overview of the conceptual framework, as well as some of the field-based methods, used in these studies. Colluvial soil is also termed regolith and although creep *sensu stricto* may occur across a wide variety of landforms and sediment types, the authors focus on hilly landscapes in this chapter.

7.13.1 Introduction

Soil creep is the most widespread and perhaps the most poorly understood process of erosion on soil-mantled hillslopes. Soil is slowly 'stirred' by burrowing creatures and uprooting vegetation; particles are also displaced in wetting–drying and freezing–thawing cycles. These actions can cause gravity-driven, downslope creep by processes that are considered to be analogous to particle diffusion (Culling, 1963; Kirkby, 1967; Roering, 2004; Foufoula-Georgiou et al., 2010; Tucker and Bradley, 2010). Other possible transport mechanisms moving soil off smoothly convex-up landscapes include shear and viscous-like creep, such that a precise characterization of the entire process appears to require the tracing of labeled soil grains (Heimsath et al., 2002). Hillslope soils are typically produced from weathering breakdown of the underlying bedrock (Carson and Kirkby, 1972; Dietrich et al., 1995; Heimsath et al., 1997), and in areas free from glacial and aeolian processes, these parent-material-derived soils contribute sediment to channels and provide habitat for much of the Earth's biota. Setting aside landslides, which are likely to dominate soil erosion in steep terrain, soil moves slowly downhill by creep and slope wash. It is especially important to acknowledge that the colluvial soils that are the focus of this chapter differ significantly from the pedogenic soils of low-lying and flat landscapes that are the focus of other studies (**Figure 1**). Quantifying the processes of soil creep on hilly and mountainous landscapes, both in terms of the best mathematical representation of the process and in terms of the actual rates of transport, is the focus of this chapter.

Early thinking about how hilly, upland landscapes evolve with time recognized that landscape morphology likely reflects the long-term dominant process shaping the landscape (Davis,

Heimsat, A.M., Jungers, M.C., 2013. Processes, Transport, Deposition and Landforms: Quantifying Creep. In: Shroder, J. (Editor in Chief), Marston, R.A., Stoffel, M. (Eds.), Treatise on Geomorphology. Academic Press, San Diego, CA, vol. 7, Mountain and Hillslope Geomorphology, pp. 138–151.

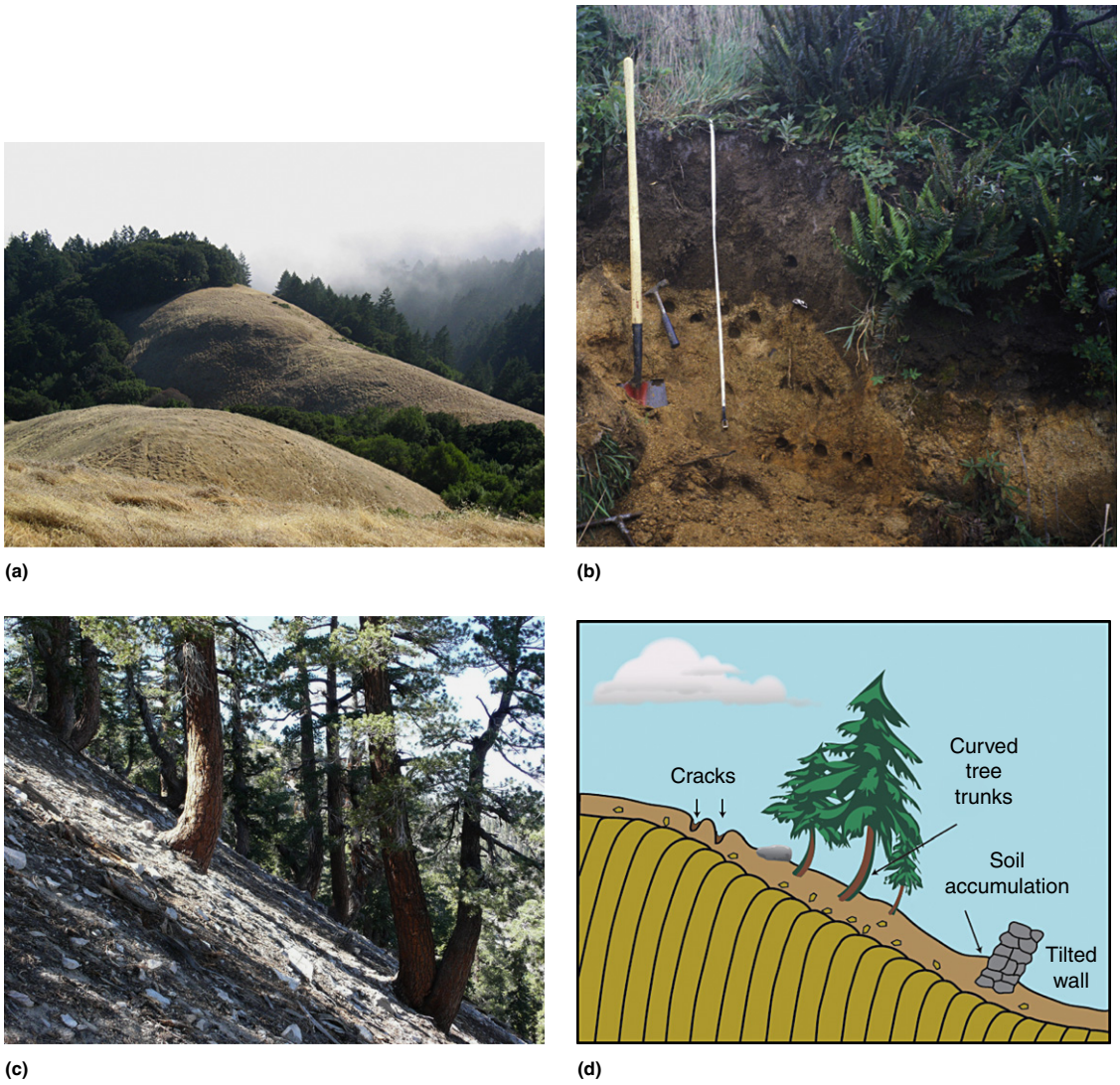

Figure 1 (a) Photograph of typical soil-mantled hillslope used for studies such as those covered in this chapter. This one is from Point Reyes, CA, during the late summer dry season. (b) Photograph of the well-mixed colluvial soil that mantles the same landscape enriched with organic matter and quite moist during the winter rains. Note the well-defined boundary between the physically mobile soil (dark layer) and the underlying weathered bedrock that retains relict rock structure and is considered to be in place. Holes are from bulk density sampling. (c) Photograph of the bent-trunk trees thought to be qualitatively indicative of creeping soils as illustrated in (d). Photograph is of a steep, stony slope in the San Gabriel Mountains, CA. (d) Cartoon adapted from typical introductory geomorphology text showing the various qualitative clues that have been used to designate creep as a dominant process. Adapted with permission from Selby, M.J., 1993. Hillslope Materials and Processes. Oxford University Press, Oxford, 451 pp.

1892; Gilbert, 1909). Specifically, the observation that smooth hillslopes tended to steepen with increasing distance from the drainage divide led to the assumption that sediment transport flux, which must increase with increasing distance from the divide, is proportional to the topographic gradient. This led to the linear transport relationship, which became known as the 'diffusion equation' because of its similar form to Fick's Law of heat diffusion. Because creep processes were considered to be responsible for transport that could be modeled as 'diffusive,' the term 'diffusion' became synonymous with creep. Recently, more accurate terms such as 'diffusion-like' or 'linear transport relationship' have been favored since soil particles are not actually diffusing downhill. They are, however, moving in a creep-like way as gravitational force imparts a downslope preference to any physical disruption of the soil.

Observations from convex hills do show that soil thickness decreases with increasing topographic curvature, supporting the view that creep occurs by diffusion-like processes with sediment flux linearly proportional to surface slope (Young, 1960; Carson and Kirkby, 1972; Heimsath et al., 1999). Such movement of individual soil grains could be caused by burrowing creatures (worms, ants, gophers, etc.) and by tree throw (trees uprooted, typically by high winds, commonly carry soil and bedrock attached to the root wad) coupled with localized rain splash and slope wash, but field observations and laboratory studies showed that nondiffusive processes may also occur,

including shear- and depth-dependent viscous-like flow (Young, 1960; Carson and Kirkby, 1972; Fleming and Johnson, 1975; Selby, 1993), as well as freeze–thaw processes (Anderson, 2002). Furthermore, the relationships observed between soil depth and slope curvature on linear and compound slopes are incompatible with a simple linear relationship between sediment flux and surface slope alone (Roering et al., 1999; Heimsath et al., 2000; Braun et al., 2001).

Rods, blocks, and flexible tubes inserted into the soil have been used to estimate creep processes (Young, 1960; Fleming and Johnson, 1975), but are too cumbersome to examine grain-scale sediment transport, which requires the use of labeled particles (Selby, 1993). Insertion and detection of labeled grains throughout a soil mantle with microscale positional measurements would be a massive undertaking (Cox and Allen, 1987; Cox, 1990; Nichols, 2004). Assuming, however, that grains brought to the surface by bioturbation and tree throw are buried again, vertical mixing at the grain scale may be determined by measuring the time since individual soil grains last visited the surface. This was done by single-grain optical dating, which is based on an optically stimulated luminescence (OSL) signal that accumulates within buried quartz grains and is reset to zero by exposure to sunlight (Heimsath et al., 2002). The resource intensity of using OSL to track soil movement led to the recent application of fallout-delivered, short-lived isotopes (^{137}Cs and ^{210}Pb) to quantify creep processes across upland landscapes (Kaste et al., 2007; O'Farrell et al., 2007; Dixon et al., 2009). In addition, fallout-delivered (or garden variety) ^{10}Be can be used to quantify hillslope sediment transport processes over longer timescales (Monaghan et al., 1983; McKean et al., 1993; Jungers et al., 2009). This chapter will explore conceptual models for creep as well as the methods used to quantify the rates and physical processes resulting in downslope soil movement on hillslopes thought to be eroding by creep. Landscape evolution models using creep as the dominant process are deliberately not examined here as these have been explored elsewhere (see, e.g., Kirkby (1971), Dietrich et al. (1995), Fernandes and Dietrich (1997), and numerous papers since then).

7.13.2 Conceptual Models for Creep

There is little need for a detailed description and elaboration on early models for creeping soil because of the lucidity of textbook presentations (Carson and Kirkby, 1972; Selby, 1993). The conceptual framework used here is based on the equation of mass conservation for physically mobile soil overlying its parent material (Carson and Kirkby, 1972; Dietrich et al., 1995). Typically, the boundary between soil and the underlying weathered (or fresh) bedrock is abrupt and can be defined within a few centimeters (**Figure 1(b)**). Soil is produced and transported by mechanical processes, and soil production rates decline exponentially with depth (Heimsath et al., 1997, 2005). The transition from soil-mantled to bedrock-dominated landscapes occurs when transport rates are higher than production rates (Anderson and Humphrey, 1989) and two transport functions are typically used to model landscape evolution (Braun et al., 2001; Dietrich et al., 2003). The slope-dependent transport law has its basis in the characteristic form of convex, soil-mantled landscapes assumed to be in equilibrium and has some field support (e.g., McKean et al., 1993; Roering et al., 2002). A nonlinear, slope-dependent transport law also has its roots in morphometric observations and has recent support, given the veracity of assuming landscape equilibrium (Roering et al., 1999), experimental constraints (Roering et al., 2001b), or postfire ravel (Gabet, 2003; Roering and Gerber, 2005).

Mechanistically, soil transport should depend on soil thickness as well as slope, as suggested by quantification of freeze–thaw (e.g., Anderson, 2002; Matsuoka and Moriwaki, 1992), shrink–swell (e.g., Fleming and Johnson, 1975), viscous or plastic flow (e.g., Ahnert, 1967), and bioturbation processes (e.g., Gabet, 2000). In each of these cases, the physical disturbance processes influence the mobile soil thickness and modulate soil transport by setting the magnitude of slope-normal displacement. The topographic gradient, or slope, influences the downhill component of the gravitational driving force. Depth-dependent flux is also suggested by the velocity profiles from segmented rod studies and modeling (Roering, 2004; Young, 1960, 1963b). The proportionality of flux to the depth-slope product is an idea that has only recently been tested despite being suggested almost 40 years ago (Ahnert, 1967; Heimsath et al., 2005; Roering et al., 2007). The differences between these potential models for creeping soil are expressed in the mathematical representation of the specific process. Each hypothesized relationship between sediment transport flux and the parameters considered to govern it yields a different equation that can be used in any model.

The form of the relationship between flux and slope, depth-slope, or slope divided by a threshold slope (i.e., nonlinearly slope-dependent) becomes important in the context of a mass balance approach to modeling landscape evolution. The development and application of this conceptual framework is well reviewed (Dietrich et al., 2003) and only summarized here to help establish how the different expressions for the flux term play a role in such models. In general, landscapes such as those shown in **Figure 1** can be represented by a conceptual model illustrated in **Figure 2** and can then be modeled using a mass conservation expression for a vertical column of soil, h, such as

$$\rho_s \frac{\partial h}{\partial t} = -\rho_r \frac{\partial z_b}{\partial t} - \nabla \tilde{q}_s \qquad [1]$$

where the vertical lowering rate of the soil-bedrock boundary, $-\partial z_b/\partial t$, at any point on the landscape is equivalent to the slope-normal soil production rate times the secant of the slope angle (Heimsath et al., 2001). The densities of the parent material, ρ_r, which can be rock or saprolite, and soil, ρ_s, are based on field measurements. If local steady-state conditions apply, that is, assuming that soil thickness at any point is constant (i.e., $\partial h/\partial t = 0$), then eqn [1] reduces to a simple relationship between vertical soil production and the divergence of sediment transport,

$$\rho_r \frac{\partial z_b}{\partial t} = -\nabla \tilde{q}_s \qquad [2]$$

It is this simple relationship that highlights the importance of the transport term. It should be noted, however, that this solution depends on the generally well-justified assumption of

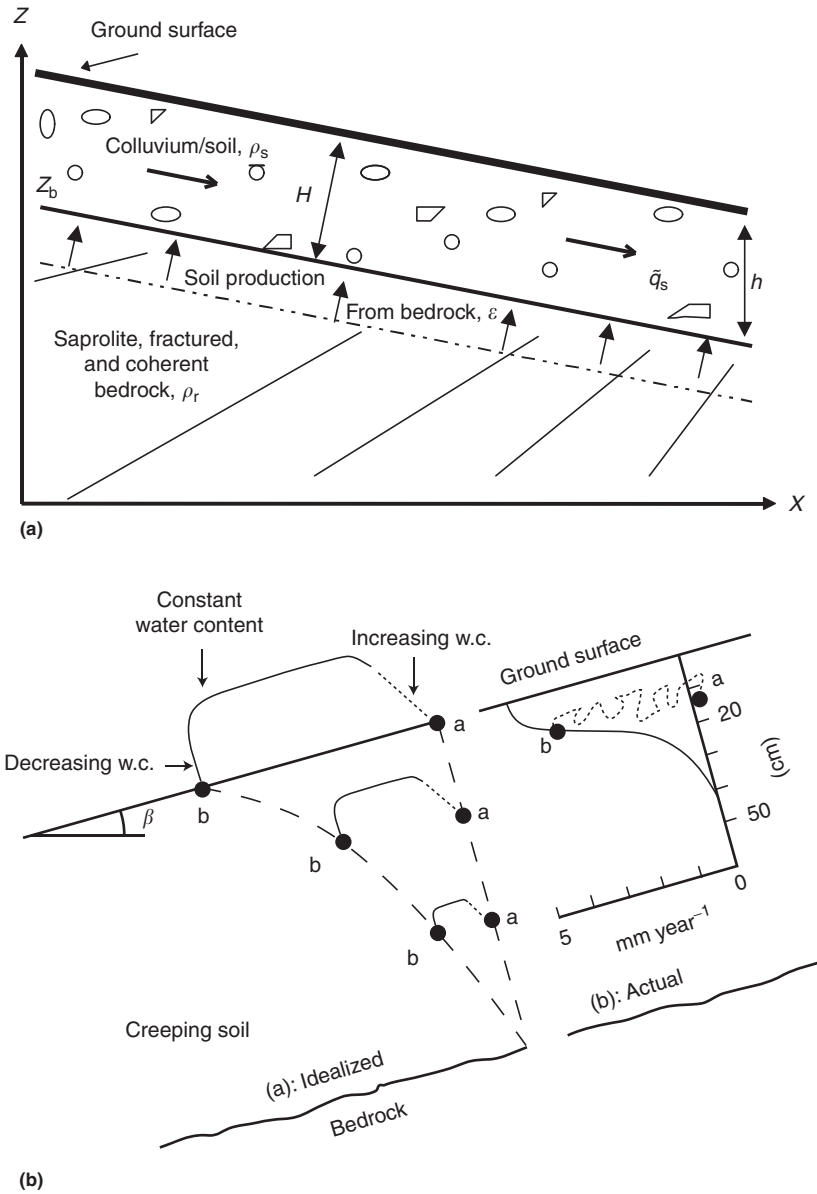

Figure 2 (a) The conceptual framework as used by Heimsath et al. (1997) studies for vertical soil depth, *h* showing how the slope-normal depth, *H*, is equal to the vertical depth times the secant of the slope angle. The change in soil mass in a column of soil with time is equal to the vertical production of soil from the underlying bedrock less the divergence of sediment transport, as described by eqn [1] in the text. (b) Idealized displacement profile (a) showing how soil particles might move from a to b in a 'laminar flow' path envisioned by Fleming and Johnson (1975) and sketched here in the text by Selby (1993). The inset (b) shows Selby's sketch of the commonly recognized 'chaotic' flow path of soil particles that may be mixed while the soil profile is shrinking and swelling from changing water content.

a steady state and that there are many soil-mantled upland landscapes where this assumption may not hold (Phillips et al., 2005; Phillips, 2010). Naturally, if the transport flux is a simple, linear function of slope as initially suggested by Gilbert and Davis and subsequently assumed by almost a century of work, then eqn [2] simplifies to the expression that led to the shorthand expression 'diffusion' when describing creep processes. Namely, flux is written to be proportional to slope,

$$\tilde{q}_s = -\rho_s K \nabla z \qquad [3]$$

where K is the transport coefficient with dimensions L^2T^{-1} and z is the ground surface elevation. When eqn [3] is substituted into eqn [2], the familiar 'diffusion' expression is derived:

$$\frac{\partial z_b}{\partial t} = -\frac{\rho_s}{\rho_r} K \nabla^2 z \qquad [4]$$

The form of eqn [4] would differ significantly depending on the most appropriate expression for the transport term, eqn [3], as well as the expression for the soil production term on the left-hand side of the equation (Roering et al., 2001a; Heimsath et al., 2005, 2009; Roering, 2008). The simplicity of these equations explains why so much effort is expended into quantifying the form of both the transport flux term and the soil production

term for this mass conservation approach. Despite the analytical simplicity, the sketch for potential paths taken by grains of soil shown in **Figure 2(b)** illustrates how complex a complete understanding of creeping soil is likely to be (Heimsath et al., 2002). In the case shown here, where sediment transport flux is linearly proportional to slope and the local soil thickness is considered to be temporally constant, one critical result expressed by eqn [4] is that the rate of soil production, which is equivalent to the rate of land-surface lowering, is a simple function of topographic curvature. For this reason alone, the linear transport function, analogous to creep, was widely assumed and extensively used in analytical and numerical models of landscape evolution (Culling, 1960, 1963; Kirkby, 1967, 1971; Armstrong, 1987; Koons, 1989; Kooi and Beaumont, 1994; Tucker and Slingerland, 1994; Dietrich et al., 1995).

More recently, the linear transport model for creeping soil was used to help test the hypothesis that soil production decreased with increasing overlying soil thickness (Heimsath et al., 1997). Equation [4] sets the rate of soil production equal to a function of the topographic curvature. Detailed measurements of the topography of numerous soil-mantled landscapes (**Figure 3(a)**) were used to calculate curvature across these landscapes (**Figure 3(b)**). The thickness of the physically mobile soils was measured in pits, locations shown for an example by the black circles on **Figure 3(a)**. Plotting curvature against soil depth (**Figure 4**) helped test the relationship between soil production and soil thickness. Morphology and a simple function for creeping soil thus helped support the soil production function, which was fully quantified using *in situ* produced cosmogenic nuclides. The fully quantified soil production function, combined with the most appropriate transport equation (e.g., eqn [3]), enables solving the governing mass balance equation and is commonly used to model landscape evolution (e.g., Dietrich et al., 1995, 2003).

7.13.3 Quantifying Creep

7.13.3.1 Physical Tracers

An innovative and not often repeated study attempting to quantify soil creep using physical tracers was published in *Nature* over half a century ago (Young, 1960). The study recognized the importance of quantifying rates and processes of hillslope denudation and set about doing this by initially inserting metal pegs into the ground surface at regular intervals downhill from a bedrock outcrop, noting the distances carefully (**Figure 5(a)**) and tracking the surface movement of clasts over time. The uncertainty involved with peg surface displacement was huge, and the problem with discerning surface transport from downslope movement occurring within the soil profile led to a modification of the method to develop what became known as a 'Young Pit.' In the first style of pit, reference pegs are inserted into the immobile rock beneath the mobile soil and a line of 10 cm metal rods is inserted into the soil profile, normal to slope, exposed on the side of the pit (**Figure 5(b)**). The second style of pit inserts the metal rods relative to a plumb bob suspended from the surface of the pit (**Figure 5(c)**). In both cases, the pit must then be filled in and the soils must be 'allowed' to erode by creep for some length of time. The pit must then be excavated and the position of the pegs carefully measured relative to the known reference frame. Despite two publications in *Nature* (Young, 1960, 1963a), few studies have followed the lead of this challenge (e.g., Schumm, 1967; Finlayson, 1981; Clarke et al., 1999), including a modified approach (Richards and Humphreys, 2010) that yielded results no less equivocal. Even the results of Schumm (1967), often cited as one of the few field-based studies confirming the linear transport relationship of eqn [3], show considerable scatter and were collected over a 7-year period,

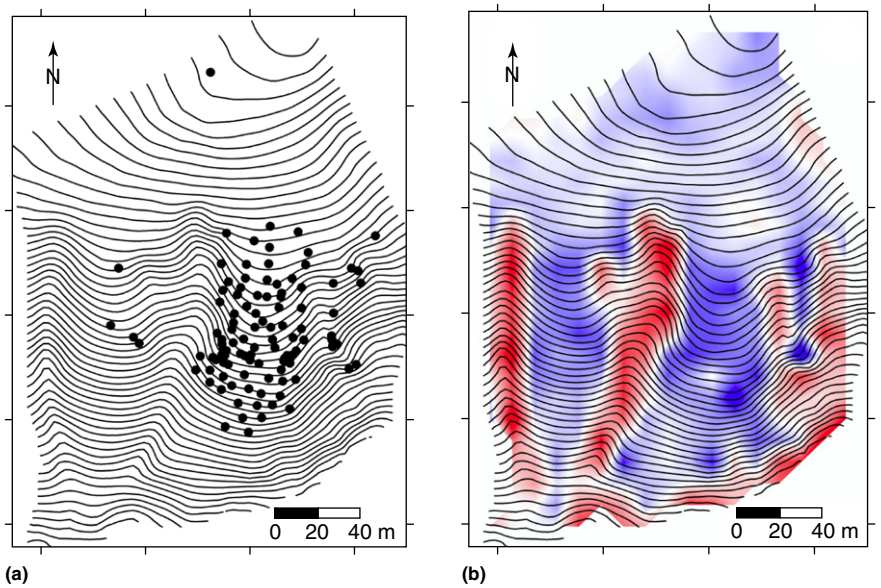

Figure 3 (a) Topographic map, 2 m contour intervals by laser total station survey, showing soil pit locations for the Pt. Reyes, CA, site of Heimsath et al. (2005). Creek drains right to left at page bottom, and elevation of the crest is 195 m. (b) Curvature map for the same surveyed area calculated using the methods of Heimsath et al. (1999): blue represents convex and red represents concave topography. Similar maps for the other soil-mantled sites used by Heimsath et al. (1997, 1999, 2000).

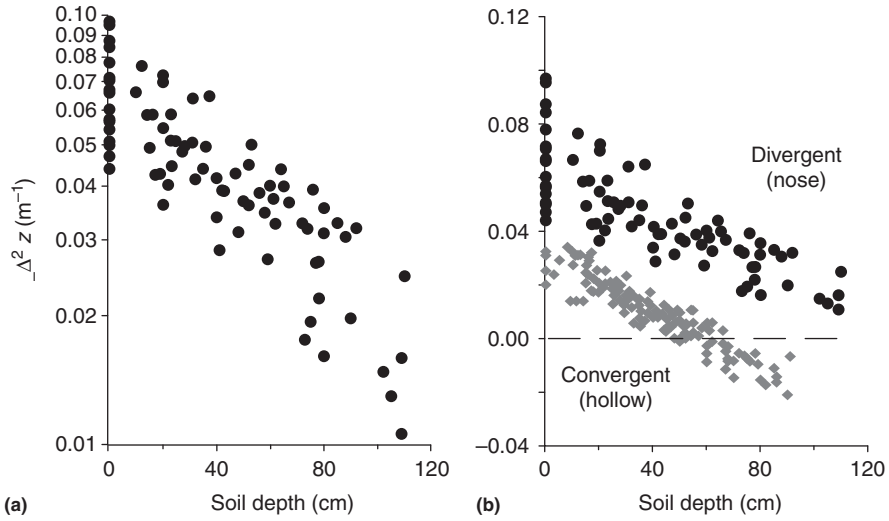

Figure 4 Negative curvature vs. vertical soil depth. Curvature calculated as in Heimsath et al. (1999) and is a proxy for soil production if the local soil depth is constant with time. (a) Black circles from individual soil pits at Pt. Reyes with an exponential negative curvature axis. (b) Black circles (as in a) with open gray diamonds that are from Nunnock River, southeastern Australia (Heimsath et al. (2000). Tennessee Valley data from Heimsath et al. (1997, 1999) overlay Nunnock River data values and range and are not included here for plot clarity. The black dashed line separates divergent from convergent topography.

longer than most are willing to devote to a single study, to say nothing of a student's PhD project. Given the results (or lack thereof) from the two most recent studies (Clarke et al., 1999; Richards and Humphreys, 2010), few others have attempted to follow Andrew Young's inspirational lead.

Fortunately, geochemical methodological advances have enabled the direct quantification of creep processes and rates with significantly less uncertainty and physical effort. Before covering the various geochemical methods used to quantify creep, another innovative approach that requires using a physical tracer and does not involve anthropogenic disturbance (i.e., the digging of numerous Young Pits) is worth summarizing. Of course, this physical tracer method also involves using geochemistry, as the studies rely on relatively precise geochemical dating (using calibrated ^{14}C dating) of tephra deposits in upland soils. Two recent studies documented profiles of tephra concentrations in hillslope soils and combined a detailed mapping of these concentrations with topographic derivatives to quantify soil transport processes (Roering et al., 2002; Walther et al., 2009). In both cases, one on a series of incised fluvial terraces along the Charwell River, South Island, New Zealand (Roering et al., 2002), and the other along a hillslope transect in the Blue Mountains, SE Washington state, USA (Walther et al., 2009), the tephra deposits are well dated and are treated as marker beds in the hillslope soils. Both studies involved extensive sampling of soil pits and auger profiles to quantify tephra distributions in the hillslope soils. Because the sample locations were located along profiles characterized by the topographic properties supporting linear transport relationships (**Figure 6**), the topographic derivatives were used with tephra distribution and concentration to provide calibrated transport relationships for each field site. Given the paucity of such field-based data supporting transport relationships, these studies are especially important. Given how difficult it is to find such ideal field locations where there are both well-dated tephras and hillslopes of characteristic form, such an innovative method is unlikely to be broadly used.

7.13.3.2 Fallout Short-Lived Isotopes

A technically less cumbersome approach involves using short-lived isotopes measured in bulk soil samples that can be collected without any disruption (i.e., by inserting tracers) and without any special site characteristics (i.e., dated tephra layers). These fallout-derived radionuclides are used extensively in erosion and sediment transport studies on both agricultural and forested landscapes. Atmospherically delivered ^{210}Pb and weapons-derived ^{137}Cs can be used alone or simultaneously to quantify and trace erosional processes (Wallbrink and Murray, 1996; Walling and He, 1999a,b; Whiting et al., 2001). The relative rates of soil mixing can be evaluated through measurements of nuclide activities in soil profiles (Dorr, 1995; Tyler et al., 2001; Kaste et al., 2007; Dixon et al., 2009). Because these isotopes are deposited at the soil surface, mixing processes can increase the dispersion of nuclides with depth and the overall downward transport rate. For example, on agricultural landscapes, where tilling homogenizes the soil to the depth of the plow layer, a unique, well-mixed ^{137}Cs profile captures the process (Walling and He, 1999a). By measuring the vertical distribution of fallout radionuclides in soils and calculating diffusion-like coefficients, the sediment transport mechanisms and mixing rates are quantified over 10–100-year timescales.

The techniques of relating fallout radionuclide profiles and inventories to absolute and relative erosion rates rely on finding a 'noneroding' reference location to compare to eroding or aggrading sites (Lowrance et al., 1988). Measured ^{210}Pb and ^{137}Cs nuclide activities are plotted with depth in the soil profile and are used with the calculated total inventories

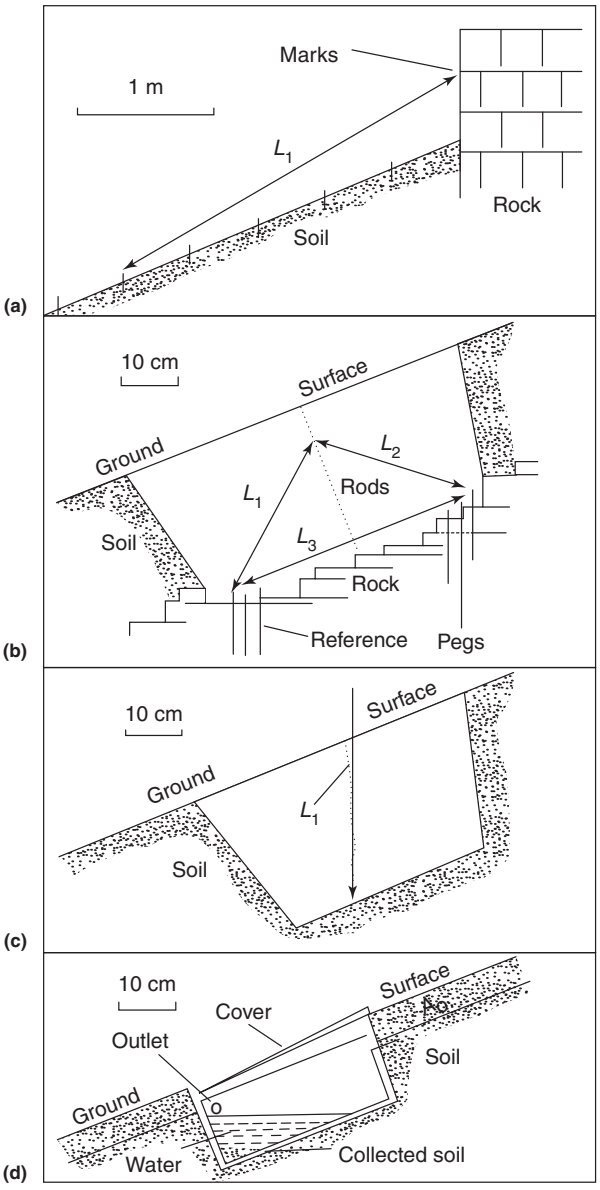

Figure 5 Concept sketch of the field techniques used to measure soil creep rates and processes ((a–c) as well as the contribution of slope wash (d) by Young (1960). The initial attempt to measure soil creep involved detailed mapping of surface clasts derived from a bedrock outcrop using pegs placed at known distances downslope from the outcrop (a). Obvious difficulties with surface disruption and peg movement led to the development of the Young Pit, which used profiles of metal rods inserted slope-normally (b) or -perpendicularly (c) into the lateral face of a soil pit. The pit would then be filled in carefully and re-excavated after a long duration of time. The metal rods would be located and their displacement would be mapped carefully relative to either pegs placed in the underlying bedrock or saprolite (b) or relative to the vertical plum line (c).

to gain an insight into mixing rates (e.g., Kaste et al., 2007; Dixon et al., 2009) and the dominant erosion mechanisms (e.g., Kaste et al., 2006; O'Farrell et al., 2007; Dixon et al., 2009). The nuclide profile depth was defined as the soil depth at which >95% of the cumulative nuclide activity, or inventory, was obtained. Nuclide profiles determine the degree of physical mixing, and a mixing coefficient can be determined by the best-fit exponential curve to an advection–diffusion equation (Kaste et al., 2007).

Two examples for how this method can be used will help illustrate its applicability to quantifying soil transport processes and rates. First, Kaste et al. (2007) measured depth profiles of ^{210}Pb across undisturbed hillslopes previously predicted (Heimsath et al., 2000, 2005) to be eroding by transport processes dominated by creep. Different shapes of the ^{210}Pb profiles quantified how soil transport transitioned from mixing-dominated across the convex crests to overland-flow-dominated near the unchanneled valley axes (**Figure 7**). Specific fits of the advection–diffusion equation enable mixing timescales to be determined for profiles, like **Figure 7(a)**, determined to be dominated by mixing that are typically near the crests of convex-up hillslopes. Conversely, for profiles in pits approaching (**Figure 7(b)**) or in (**Figure 7(c)**) the convergent swale, the proportion of sediment likely to be removed by overland flow processes can be quantified by comparing the profile in **Figure 7(c)** with the profile shown in **Figure 7(a)**, for example. Furthermore, using short-lived isotope profiles such as the ones shown in **Figure 7**, along with longer (i.e., millennial) timescale measurements of erosion rates, supported the temporal steady-state assumption for three well-studied field sites (Kaste et al., 2007).

The second example used a similar approach for analyzing the short-lived isotope profiles, but combined them with longer timescale measurements of soil production and average erosion rates using *in situ* produced cosmogenic ^{10}Be. Dixon et al. (2009) used both ^{210}Pb and ^{137}Cs to quantify the differences in erosional processes and rates across two sites at the climatic extremes in the Sierra Nevada Mountains of California. Penetration depths of both nuclides increased linearly in soils with burrowing activity at both sites, suggesting that bioturbation redistributes nuclides to depth in the soil. Assuming nuclide profiles form primarily by diffusion-like, (i.e., creep) processes, the average mixing coefficients of soils at the low-elevation, oak-grassland sites were significantly higher than at the high-elevation, alpine site. Total ^{210}Pb inventories did not vary across the low-elevation site; however, at the high-elevation, snow-dominated site, inventories were lowest where slopes are steepest and had the greatest upslope contributing area. The strong correlation of nuclide inventory with the upslope contributing area suggested that overland flow plays an important role at the higher elevation site (**Figure 8**), where snowmelt and the relative absence of vegetation were likely to shift the dominant creep process away from bioturbation-driven soil mixing. The results from both these studies, and others like them that use short-lived isotopes to track sediment transport, led to significant advances in understanding and calibrating creep processes, but they all rely on the use of expensive instruments and careful processing of the isotopic data.

7.13.3.3 Meteoric ^{10}Be

Meteoric ^{10}Be is a cosmogenic radionuclide well suited for use as a tracer of soil creep over geomorphic timescales. Spallation

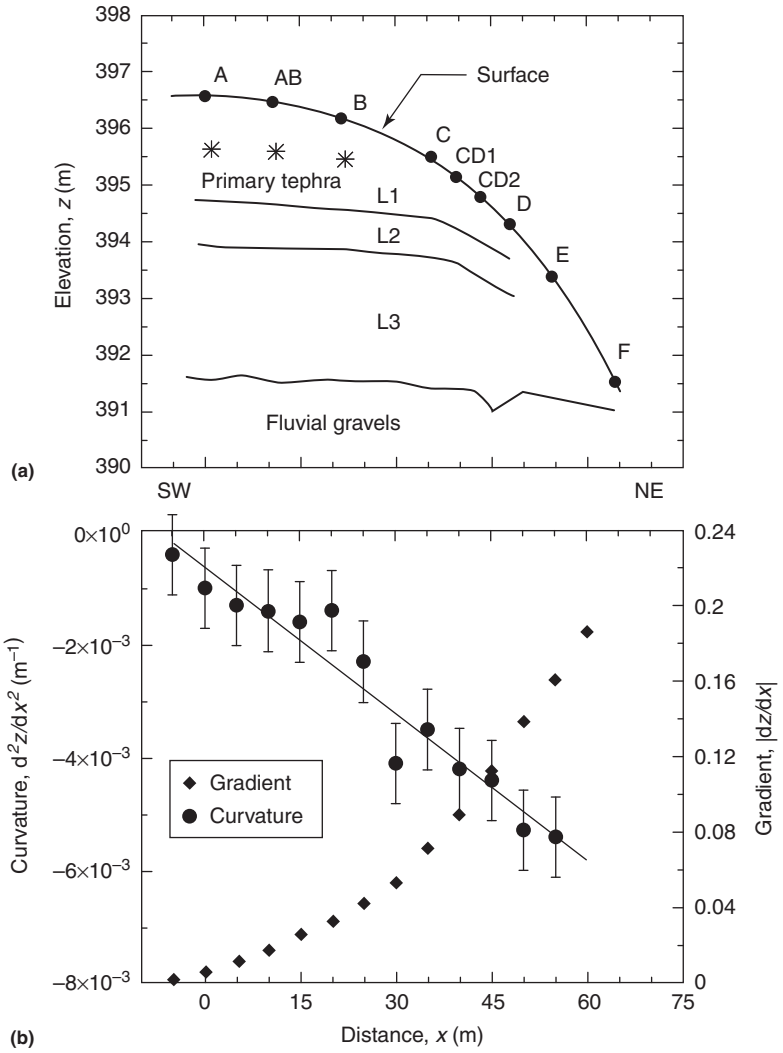

Figure 6 Morphology of the hillslope studied by Roering et al. (2002). (a) Profile of the hillslope surface elevation (convex-up curve) showing, with black-filled circles, the locations of continuous auger samples used to map tephra distribution in the soil profiles. The letters on top of the sample locations designate the profiles discussed in detail in their paper. The three loess units deposited on top of coarse fluvial gravels denoted by L1, L2, and L3 at appropriate elevations. (b) Profiles of hillslope gradient (black-filled stars) and curvature (black-filled circles) with distance downslope using the same *X* axis as (a) and showing one standard error in curvature estimation.

of oxygen and nitrogen in the Earth's atmosphere produces the majority of ^{10}Be present in natural systems (Lal and Peters, 1967). Following production, ^{10}Be is delivered to the Earth's surface at a rate most significantly proportional to regional precipitation fluxes (Graly et al., 2011). A smaller, but not insignificant, inventory of ^{10}Be falls from the atmosphere adsorbed to terrestrial dust (Willenbring and von Blackenburg, 2010; Graly et al., 2011). The timescale over which any radioactive tracer is useful is a function of the rate at which the isotope is produced and delivered to the natural system of interest and of the rate at which the radionuclide decays. ^{10}Be has a half-life of 1.39×10^6 years (Korschinek et al., 2010), making it especially useful as a tool for quantifying rates of Earth surface processes that take place over thousands to millions of years. Additionally, ^{10}Be adsorbs quickly and strongly to soil particles (You et al., 1989), and a soil mantle's total ^{10}Be inventory can reliably be accounted for if samples integrate from the soil–atmosphere interface to the contact between soil/saprolite and unweathered bedrock (Graly et al., 2010). Naturally, it follows that landscapes with relatively thin (0–150 cm) soil mantles are most amenable to the task of capturing complete ^{10}Be inventories (**Figure 9**).

Monaghan et al. (1992) measured meteoric ^{10}Be depth profiles within 1–2-m-thick clay-rich soils mantling convex hillslopes of coastal California. In addition to being convex, this study's hillslopes showed no evidence for erosion by overland flow, and evidence for landsliding was present only low on the slopes. In such a landscape, the dominant mechanism for hillslope sediment transport is soil creep, and erosional processes should abide by transport laws similar to the linear diffusion model outlined earlier in this chapter. Monaghan et al. (1992) thus considered their results in the context of

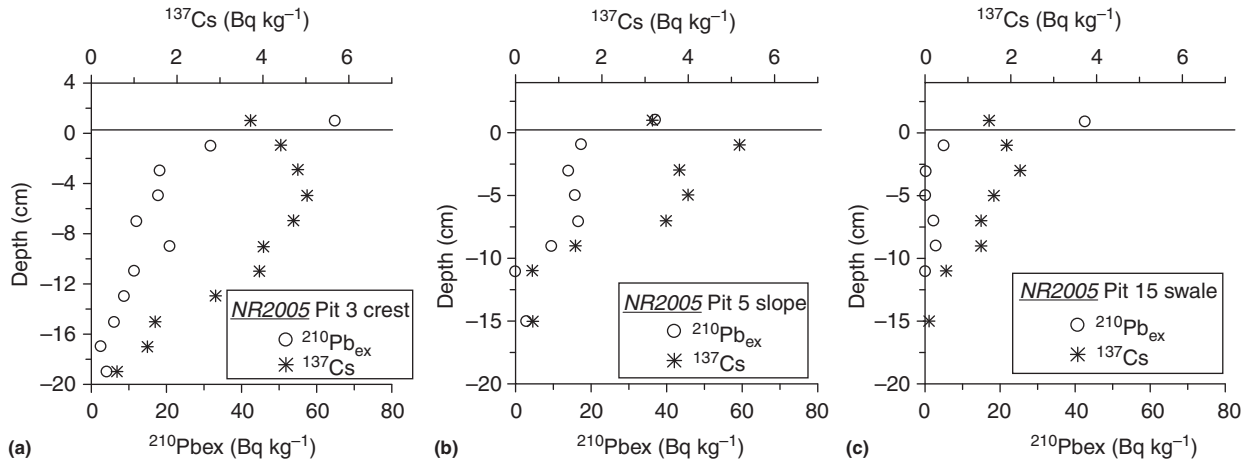

Figure 7 Short-lived isotope profiles from crest (a), midslope (b), and unchanneled swale (c). Open circles show the activities of ^{210}Pb with depth in the profiles, whereas the asterisk symbols show the activities of ^{137}Cs with depth from the same samples. Greater depth penetration of the short-lived isotopes in (a) used to quantify more extensive mixing from bioturbation using an advection–diffusion equation to fit the data. Both the depth penetration and the total isotope activity integrated over the entire profile decline with distance downslope showing the increasing dominance of overland flow to remove the surface, nuclide-rich soils as shown, for example, in (c).

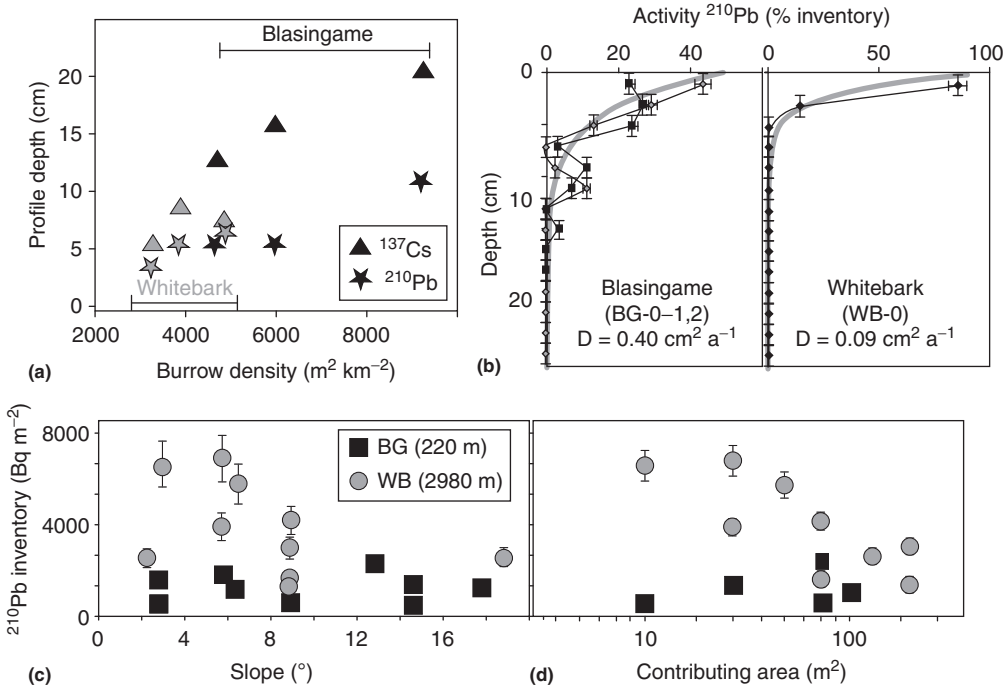

Figure 8 (a) Surface burrowing activities from three transects at low-elevation Blasingame (BG) and high-elevation Whitebark (WB) increase with associated profile depths for fallout nuclide ^{210}Pb and ^{137}Cs. (b) Fallout profiles show nuclide activity vs. depth for hillcrests at BG and WB and are deeper at BG. The diffusion-like mixing coefficients for each profile (shown by broad gray line) were calculated by the best fit to the advection–diffusion equation of Kaste et al. (2007), assuming that the advection velocity is zero. Diffusive mixing coefficients of hillcrests are shown in the figure, and the average hillslope values at each site are 0.28 ± 0.05 cm^2 yr^{-1} at BG and 0.15 ± 0.02 cm^2 yr^{-1} at WB. Inventories (c, d) of ^{210}Pb excess and ^{137}Cs for downslope soils at low-elevation BG (gray squares) and high-elevation WB (black circles). Inventory data points reflect those calculated from individual soil profiles and activities of additional bulk soil samples gathered downslope. (c) Nuclide inventories at high elevation are lower at high slopes, suggesting increased removal of soil. (d) At BG, inventories do not change markedly; whereas at WB, nuclide inventories decrease with distances downslope and increasing contributing area. Symbols contain error if not otherwise labeled. Adapted from Dixon et al. (2009).

Gilbert (1909) and investigated whether the rate of regional uplift is in equilibrium with local rates of bedrock-to-soil conversion coupled to the rate of the dominant soil transport mechanism, soil creep. Soil residence times inferred from the ^{10}Be inventories of hillslope soils were two orders of magnitude lower than the soil residence times on geochemically comparable stable surfaces. The authors attribute this difference to the steady removal of mass and ^{10}Be from eroding surfaces

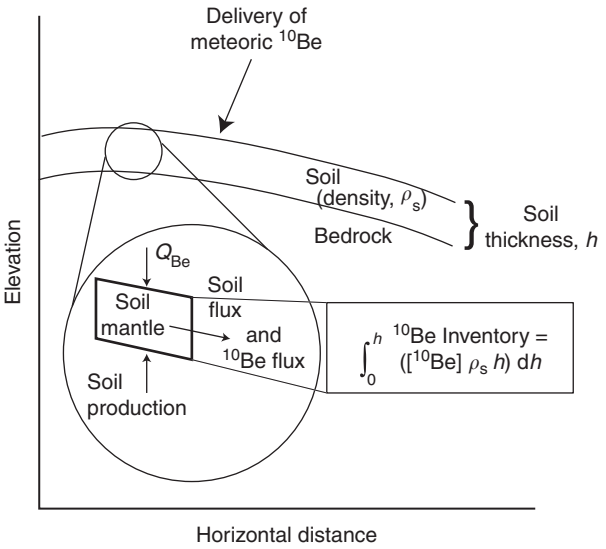

Figure 9 Schematic cross section of a soil-mantled hillslope. A mass and isotope balance for the soil mantle at any point on the hillslope includes: flux of ^{10}Be delivered from the atmosphere; flux of mass from soil production at the bedrock soil contact, $h=0$, generally very low in ^{10}Be activity; flux of mass and ^{10}Be from upslope soil. A ^{10}Be inventory for any portion of the soil mantle integrates the concentration of ^{10}Be adsorbed to soil from the bedrock–soil interface (or where [^{10}Be]$=0$) to the soil–atmosphere interface. Modified from McKean et al. (1993).

via soil creep. Assuming steady-state erosion, Monaghan et al. (1992) used a mass and isotope balance to show that rates of bedrock-to-soil conversion (g cm^{-2} yr^{-1}) may be calculated using the ratio of ^{10}Be delivery to the system (atoms cm^{-2} yr^{-1}) to the concentration of ^{10}Be removed by soil creep (atoms g^{-1}). Notably, the average rates of soil production were $\sim$0.2 mm yr^{-1}, which is in agreement with coastal uplift rates of $\sim$0.3 mm yr^{-1} (McLaughlin et al., 1983), strengthening their argument for steady-state conditions. Holding soil density and soil mantle thickness constant, the authors calculated an average, creep-driven soil transit time from hillcrest to hollow of $\sim$12 500 years for this landscape.

McKean et al. (1993) built directly upon the methodological foundation established by Monaghan et al. (1992), but they added the explicit consideration of hillslope gradient in their study in order to further test the conceptual model of hillslope sediment transport according to a linear diffusion-like transport law. These authors collected meteoric ^{10}Be profiles in three pits along a one-dimensional topographic transect from hillcrest to midslope. Soil flux via soil creep increased with increasing surface gradient (i.e., distance from the hillcrest because the hillslope was convex), and a diffusion coefficient of 360 ± 55 cm^3 yr^{-1} cm^{-1} defined the relationship. A noteworthy reviewer's comment by Robert Anderson written at the end of McKean et al. (1993) regarded this study as "The first direct test of the applicability of a long-revered analysis of Gilbert's."

Jungers et al. (2009) traced hillslope sediment transport using both meteoric and *in situ* produced ^{10}Be in the Great Smoky Mountains, NC. The dominant transport mechanism on this study's hillslope was soil creep driven by stochastic tree throw events. Millennial scale mixing of the soil mantle by tree throw is supported by nearly uniform *in situ* ^{10}Be depth profiles to $\sim$60 cm, the average thickness of tree throw rootwards. The authors quantified sediment transport velocities by comparing soil pit ^{10}Be inventories to maximum particle path distances inferred from a 1 m resolution DEM derived from an airborne light detection and ranging data set. This approach yielded estimates for soil creep rates of 1.2–1.7 cm yr^{-1} from meteoric ^{10}Be and 1.1–1.3 cm yr^{-1} from *in situ* produced ^{10}Be. These rates translate into soil transit times of 24 000–36 000 years from the hillcrest to the bounding stream, which agrees well with soil residence times of 22 000–33 000 years inferred from meteoric ^{10}Be inventories.

7.13.3.4 OSL Dating

OSL became the established successor to thermoluminescence (TL) as the means for measuring the time elapsed since a mineral grain's last exposure to sunlight (e.g., Aitken, 1985, 1994; Huntley et al., 1985; Duller, 1996; Roberts et al., 1990, 1997). The OSL measurements from quartz and feldspar grains focus on the most light-sensitive electron traps, less readily measurable than TL. Although exposure ages can be measured from both minerals, quartz is the dosimeter of choice because the microdosimetry in feldspar grains is complex and the stored dose decays unpredictably (Murray et al., 1995). The OSL dating initially used gram-sized samples of thousands of sand grains. The second stage of development involved the 'small aliquot' methods, which used a few tens to a few hundred mineral grains per sample. The most recent and still ongoing stage of OSL development is the 'single grain' method of dating, which uses a pixel-based optical scanning system to measure the age of each grain or each very small group of grains.

Although most applications of OSL have been for dating human artifacts and sedimentary deposits, the methodology can readily be used to quantify hillslope sediment transport rates and to distinguish between different transport processes. Optical ages of grains from different depths depend on transport processes: For example, grains moving in a surface layer would intermittently be exposed to sunlight, whereas grains never exposed at the surface should show 'infinite' ages. Alternatively, mixing throughout the entire soil column would lead to finite-aged grains from the soil surface to its base, the boundary with the underlying saprolite, and the source of the mobile soil.

Downhill movement of any soil grain resolves into slope-normal and slope-parallel components. Only the slope-normal velocity of a grain can be derived from its optical age. Such methods cannot assess the slope-parallel velocity of individual grains, but the depth-averaged velocity can be calculated if the rate of soil production from rock weathering is known at all points and if the topography of the site is well constrained. Soil-production rates were previously determined from measurements of the *in situ* cosmogenic nuclides ^{10}Be and ^{26}Al (Heimsath et al., 2000) and were then used in a new way by Heimsath et al. (2002) to derive slope-parallel velocities. Additionally, modeling of the landscape evolution of the site (Braun et al., 2001) highlighted the need for a more detailed

field understanding of the sediment transport processes active on soil-mantled landscapes. Unfortunately, the resource intensity of using OSL to date individual soil grains and the attempt to fully quantify soil transport processes proved to be a significant hurdle. To date, the Heimsath et al. (2002) paper is the only application of OSL to quantifying known creep processes.

7.13.3.5 Integrating Soil Production Rates

To test and further refine the mathematical model for creeping soil, Heimsath et al. (2005) used high-resolution topography, hundreds of soil-depth measurements, and previously quantified soil production functions to quantify soil flux across three landscapes. They specifically used field-based data to test the hypothesis that sediment transport is proportional to the product of soil depth and topographic gradient (rather than the gradient alone, as in eqn [3]). Using soil production rates quantified with *in situ* produced ^{10}Be and the mass-balance approach of eqn [1], Heimsath et al. (2005) plotted depth-integrated flux against the depth-slope product across three different field areas to test the nonlinear transport law embodied by the depth-slope product (**Figure 10(a)**). They observed linear increases of soil flux with increasing depth-slope product for both the Nunnock River and the Tennessee Valley field sites, offering strong support for the depth-dependent transport relationship. Data from Nunnock River support a depth-slope transport coefficient, K_h, equal to 0.55 cm yr^{-1}. Roughly equating this coefficient to the linear 'diffusivity' with an average soil thickness for Nunnock River of 65 cm yields a coefficient of 36 cm^2 yr^{-1}, which is remarkably similar to the 40 cm^2 yr^{-1} reported by Heimsath et al. (2000). Reversing the process for the Tennessee Valley and Point Reyes data, which have independently determined linear 'diffusivities' of 50 and 30 cm^2 yr^{-1} and average soil thicknesses of 30 and 50 cm, yields depth-dependent transport coefficients of 1.7 and 0.6 cm yr^{-1}, respectively. Using the data from Tennessee Valley and Point Reyes, K_h values of 1.2 and 0.4 cm yr^{-1} were determined.

This comparison of transport coefficients places the depth-dependent transport flux within the context of the more familiar slope-dependent (i.e., creep in the traditional sense) transport framework and supports the applicability of a linear transport law for low-gradient, convex landscapes. However, plotting flux against gradient showed that a linear relationship

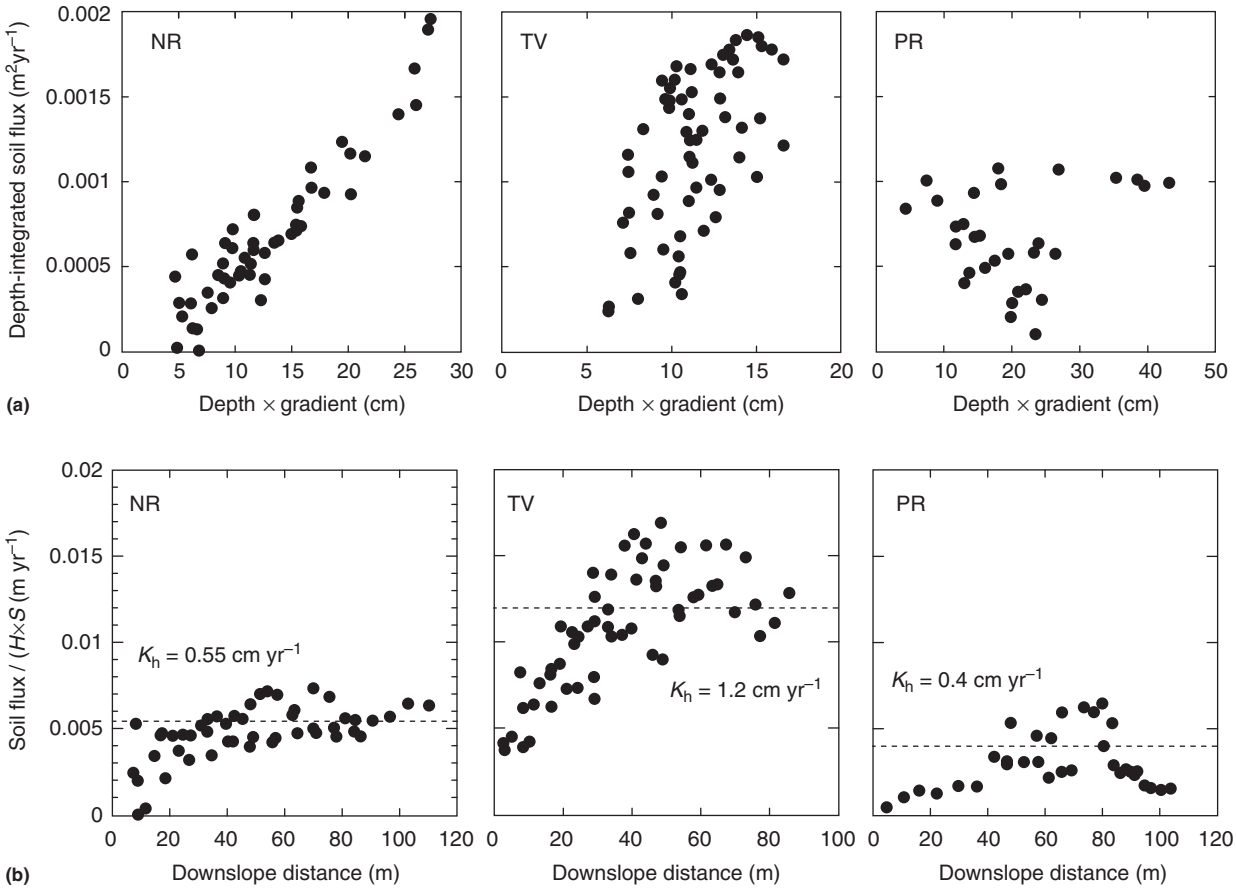

Figure 10 (a) Depth-integrated soil flux per unit contour length (m^2 yr^{-1}) vs. the depth-slope product (cm) for three study areas where soil production functions were quantified: NR – Nunnock River, southeastern Australia (Heimsath et al., 2000); TV – Tennessee Valley, CA (Heimsath et al., 1997); and PR – Point Reyes, CA (Heimsath et al., 2005). (b) Depth-integrated flux divided by depth-slope product vs. downslope distance, *X*. The K_h value, determined by fitting data shown in (a), is a dashed line. See text for the importance of (b) and the dashed line. Adapted from Heimsath et al. (2005).

does not reflect all the data. Their test for depth-dependent transport thus involved two sets of complementary plots: **Figure 10(a)** plots depth-integrated flux, $H\bar{q}_s$, versus the depth-slope product, HS, whereas **Figure 10(b)** plots $H\bar{q}_s(HS)^{-1}$ versus downslope distance, X. If a depth-slope product equation for eqn [3] is correct, the first plots (**Figure 10(a)**) would show a linear increase, with the slope of the relationship equal to K_h and having a zero origin – in the absence of covariance of H or S with distance X. However, because $H\bar{q}_s$ must (by definition) increase with distance, X, the plots might exhibit a spurious covariance with the depth-slope product. Thus, the importance of the plots in **Figure 10(b)** was to remove any such covariance such that the data should be homoskedastic about a flat line equal to K_h (dashed line) to support the depth-slope equation. Heimsath et al. (2005) observed, instead, an increase with distance close to the ridge crests, followed by a tendency to flatten roughly around the K_h values. Potential explanations for the increase include the unknown role of chemical weathering or a nonconstant, covariant transport coefficient. They concluded their analyses by suggesting that it is incorrect to think of landscapes eroding by processes termed to be diffusive, and they suggested that future landscape evolution modeling efforts more completely couple spatial variations in soil depth with soil production and transport processes.

7.13.4 Conclusion

Creep, as described in typical geomorphology textbooks, may be applied widely to describe erosional processes active across upland, soil-mantled landscapes. Quantifying creep processes and rates proves, however, to be much more difficult and resource intensive than the basic mathematical framework used to describe its conceptual framework would lead one to believe. This chapter focuses on the field-based measurements used to quantify creep after summarizing the conceptual framework and introducing the mass balance approach used to derive the mathematical analyses applied in landscape evolution models. From the incredibly physically challenging Young Pits to the incredibly expensive use of *in situ* and meteoric cosmogenic nuclides, the methods all pose challenges to those interested in peering inside the relative black box of a creeping soil. Anthropogenically introduced physical tracers used in Young Pits yield perhaps the most difficult and time-consuming results that are also likely to be the most equivocal. Use of careful mapping of dated tephras may have great potential and is a relatively inexpensive method, but the need for an ideal field site is extremely limiting. Short-lived isotopes rely on expensive and carefully calibrated equipment, but the measurements and sample preparations are easy and can be applied broadly. The results are promising, but the isotopic analyses are likely to be a significant hurdle for extensive application. The same is likely to be true, with the added challenge of a rather significant sample analyses expense, for cosmogenic nuclide as well as OSL applications. Despite all of these challenges, quantification of creep remains an important and worthwhile endeavor for a greater understanding of how the Earth's surface is evolving. Perhaps the greatest motivation for quantifying creep is the importance of being able to predict how the critical zone that is home to most of the Earth's terrestrial biota is likely to change under the changing climatic driving forces.

Acknowledgement

Much of the work reported upon here by AMH and MCJ was supported by the National Science Foundation.

References

Ahnert, F., 1967. The role of the equilibrium concept in the interpretation of landforms of fluvial erosion and deposition. In: Macar, P. (Ed.), L'evolution des Versants. University of Liege, Liege, France, pp. 23–41.
Aitken, M.J., 1985. Thermoluminescence Dating. Academic Press, London.
Aitken, M.J., 1994. Optical dating: a non-specialist review. Quaternary Science Reviews 13, 503–508.
Anderson, R.S., 2002. Modeling the tor-dotted crests, bedrock edges, and parabolic profiles of high alpine surfaces of the Wind River Range, Wyoming. Geomorphology 46, 35–58.
Anderson, R.S., Humphrey, N.F., 1989. Interaction of weathering and transport processes in the evolution of arid landscapes. In: Cross, T.A. (Ed.), Quantitative Dynamic Stratigraphy. Prentice-Hall, Englewood Cliffs, NJ, pp. 349–361.
Armstrong, A.C., 1987. Slopes, boundary conditions, and the development of convexo-concave forms – some numerical experiments. Earth Surface Processes and Landforms 12, 17–30.
Braun, J., Heimsath, A.M., Chappell, J., 2001. Sediment transport mechanisms on soil-mantled hillslopes. Geology 29, 683–686.
Carson, M., Kirkby, M., 1972. Hillslope Form and Process. Cambridge University Press, Cambridge, UK, 475 pp.
Clarke, M.F., Williams, M.A.J., Stokes, T., 1999. Soil creep: problems raised by a 23 year study in Australia. Earth Surface Processes & Landforms 24, 151–175.
Cox, G.W., 1990. Soil mining by pocket gophers along topographic gradients in a mima moundfield. Ecology 71, 837–843.
Cox, G.W., Allen, D.W., 1987. Soil translocation by pocket gophers in a mima moundfield. Oecologia 72, 207–210.
Culling, W.E.H., 1960. Analytical theory of erosion. The Journal of Geology 68, 336–344.
Culling, W.E.H., 1963. Soil creep and the development of hillside slopes. The Journal of Geology 71, 127–161.
Davis, W.M., 1892. The convex profile of badland divides. Science 20, 245.
Dietrich, W.E., Bellugi, D., Heimsath, A.M., Roering, J.J., Sklar, L., Stock, J.D., 2003. Geomorphic transport laws for predicting the form and evolution of landscapes. In: Wilcock, P.R., Iverson, R. (Eds.), Prediction in Geomorphology. AGU, Washington, DC, Geophysical Monograph Series, pp. 103–132.
Dietrich, W.E., Reiss, R., Hsu, M.-L., Montgomery, D.R., 1995. A process-based model for colluvial soil depth and shallow landsliding using digital elevation data. Hydrological Processes 9, 383–400.
Dixon, J.L., Heimsath, A.M., Kaste, J., Amundson, R., 2009. Climate-driven processes of hillslope weathering. Geology 37, 975–978.
Dorr, H., 1995. Application of 210Pb in soils. Journal of Paleolimnology 13, 157–168.
Duller, G.A.T., 1996. Recent developments in luminescence dating of Quaternary sediments. Progress in Physical Geography 20, 127–145.
Fernandes, N.F., Dietrich, W.E., 1997. Hillslope evolution by diffusive processes: the timescale for equilibrium adjustments. Water Resources Research 33, 1307–1318.
Finlayson, B., 1981. Field measurements of soil creep. Earth Surface Processes and Landforms 6, 35–48.
Fleming, R.W., Johnson, A.M., 1975. Rates of seasonal creep of silty clay soil. Quarterly Journal of Engineering Geology 8, 1–29.
Foufoula-Georgiou, E., Ganti, V., Dietrich, W.E., 2010. A nonlocal theory of sediment transport on hillslopes. Journal of Geophysical Research 115, 1–12, F00A16.
Gabet, E.J., 2000. Gopher bioturbation: field evidence for non-linear hillslope diffusion. Earth Surface Processes and Landforms 25, 1419–1428.
Gabet, E.J., 2003. Post-fire thin debris flows: sediment transport and numerical modelling. Earth Surface Processes and Landforms 28, 1341–1348.

Gilbert, G.K., 1909. The Convexity of Hilltops. Journal of Geology 17, 344–350.

Graly, J.A., Bierman, P.R., Reusser, L.J., Pavich, M.J., 2010. Meteoric Be-10 in soil profiles – a global meta analysis. Geochemica et Cosmochemica Acta 74, 6814–6829.

Graly, J.A., Reusser, L.J., Bierman, P.R., 2011. Short and long-term delivery rates of meteoric Be-10 to terrestrial soils. Earth & Planetary Science Letters 302, 329–336.

Heimsath, A.M., Dietrich, W.E., Nishiizumi, K., Finkel, R.C., 1997. The soil production function and landscape equilibrium. Nature 388, 358–361.

Heimsath, A.M., Dietrich, W.E., Nishiizumi, K., Finkel, R.C., 1999. Cosmogenic nuclides, topography, and the spatial variation of soil depth. Geomorphology 27, 151–172.

Heimsath, A.M., Chappell, J., Dietrich, W.E., Nishiizumi, K., Finkel, R.C., 2000. Soil production on a retreating escarpment in southeastern Australia. Geology 28, 787–790.

Heimsath, A.M., Dietrich, W.E., Nishiizumi, K., Finkel, R.C., 2001. Stochastic processes of soil production and transport: erosion rates, topographic variation, and cosmogenic nuclides in the Oregon Coast Range. Earth Surface Processes and Landforms 26, 531–552.

Heimsath, A.M., Chappell, J., Spooner, N.A., Questiaux, D.G., 2002. Creeping soil. Geology 30, 111–114.

Heimsath, A.M., Furbish, D.J., Dietrich, W.E., 2005. The illusion of diffusion: field evidence for depth-dependent sediment transport. Geology 33, 949–952.

Heimsath, A.M., Hancock, G.R., Fink, D., 2009. The 'humped' soil production function: eroding Arnhem Land, Australia. Earth Surface Processes & Landforms 34, 1674–1684.

Huntley, D.J., Godfrey-Smith, D.I., Thewalt, M.L.W., 1985. Optical dating of sediments. Nature 313, 105–107.

Jungers, M.C., Bierman, P.R., Matmon, A., Nichols, K., Larsen, J., Finkel, R., 2009. Tracing hillslope sediment production and transport with in situ and meteoric 10Be. Journal of Geophysical Research 114, F04020. doi:10.1029/2008JF001086.

Kaste, J.M., Heimsath, A.M., Hohmann, M., 2006. Quantifying sediment transport across an undisturbed prairie landscape using Caesium-137 and high-resolution topography. Geomorphology 76, 430–440.

Kaste, J., Heimsath, A.M., Bostick, B.C., 2007. Short-term soil mixing quantified with fallout radionuclides. Geology 35, 243–246.

Kirkby, M.J., 1967. Measurement and theory of soil creep. The Journal of Geology 75, 359–378.

Kirkby, M.J., 1971. Hillslope process-response models based on the continuity equation. Institute of British Geographers, London, Special Publication 3, pp. 15–30.

Kooi, H., Beaumont, C., 1994. Escarpment evolution on high-elevation rifted margins: insights derived from a surface processes model that combines diffusion, advection, and reaction. Journal of Geophysical Research 99, 12,191–12,209.

Koons, P.O., 1989. The topographic evolution of collisional mountain belts: a numerical look at the Southern Alps, New Zealand. American Journal of Science 289, 1041–1069.

Korschinek, G., Bergmaier, A., Faestermann, T., et al., 2010. A new value for the half-life of Be-10 by Heavy-Ion Elastic Recoil Detection and liquid scintillation counting. Nuclear Instruments & Methods in Physics Research Section B – Beam Interactions with Materials and Atoms 268, 187–191.

Lal, D., Peters, B., 1967. Cosmic ray produced radioactivity on the earth. In: Fluegge, S., Sitte, K. (Eds.), Handbuch der Physik, Band XLVI/2. Springer-Verlag, Berlin, Heidelberg, New York, pp. 551–612.

Lowrance, R., McIntyre, S., Lance, C., 1988. Erosion and deposition in a field forest system estimated using cesium-137 activity. Journal of Soil and Water Conservation 43, 195–199.

Matsuoka, N., Moriwaki, K., 1992. Frost heave and creep in the Sor Rondane Mountains, Antartica. Arctic & Alpine Research 24, 271–280.

McKean, J.A., Dietrich, W.E., Finkel, R.C., Southon, J.R., Caffee, M.W., 1993. Quantification of soil production and downslope creep rates from cosmogenic ^{10}Be accumulations on a hillslope profile. Geology 21, 343–346.

McLaughlin, R.J., Lajoie, K.R., Sorg, D.H., Morrison, S.D., Wolfe, J.A., 1983. Tectonic uplift of a middle Wisconsin marine platform near the Mendocino triple junction, California. Geology 11, 35–39.

Monaghan, M.C., Krishnaswami, S., Thomas, J., 1983. ^{10}Be concentration and long-term fate of particle-reactive nuclides in five soil profiles from California. Earth & Planetary Science Letters 65, 51–60.

Monaghan, M.C., McKean, J., Dietrich, W.E., Klein, J., 1992. 10Be chronometry of bedrock-to-soil conversion rates. Earth and Planetary Science Letters 111, 483–492.

Murray, A.S., Olley, J.M., Caitcheon, G.G., 1995. Measurement of equivalent doses in quartz from contemporary water-lain sediments using optically stimulated luminescence. Quaternary Science Reviews 14, 365–371.

Nichols, M.H., 2004. A radio frequency identification system for monitoring coarse sediment particle displacement. Applied Engineering in Agriculture 20, 783–787.

O'Farrell, C.R., Heimsath, A.M., Kaste, J.M., 2007. Quantifying hillslope erosion rates and processes for a coastal California landscape over varying timescales. Earth Surface Processes & Landforms 32, 544–560.

Phillips, J.D., 2010. The convenient fiction of steady-state soil thickness. Geoderma 156, 389–398.

Phillips, J.D., Marion, D.A., Luckow, K., Adams, K.R., 2005. Nonequilibrium regolith thickness in the Ouachita Mountains. Journal of Geology 113, 325–340.

Richards, P.J., Humphreys, G.S., 2010. Burial and turbulent transport by bioturbation: a 27-year experiment in southeast Australia. Earth Surface Processes and Landforms 35, 856–862.

Roberts, R.G., Jones, R., Smith, M.A., 1990. Thermoluminescence dating of a 50,000-year-old human occupation site in northern Australia. Nature 345, 153–156.

Roberts, R.G., Walsh, G., Murray, A., et al., 1997. Luminescence dating of rock art and past environments using mud-wasp nests in northern Australia. Nature 387, 696–699.

Roering, J.J., 2004. Soil creep and convex-upward velocity profiles: theoretical and experimental investigation of disturbance-driven sediment transport on hillslopes. Earth Surface Processes and Landforms 29, 1597–1612.

Roering, J.J., 2008. How well can hillslope evolution models "explain" topography? Simulating soil transport and production with high-resolution topographic data. Geological Society of America Bulletin 120, 1248–1262.

Roering, J.J., Almond, P., Tonkin, P., McKean, J., 2002. Soil transport driven by biological processes over millennial time scales. Geology 30, 1115–1118.

Roering, J.J., Gerber, M., 2005. Fire and the evolution of steep, soil-mantled landscapes. Geology 33, 349–352.

Roering, J.J., Kirchner, J.W., Dietrich, W.E., 1999. Evidence for nonlinear, diffusive sediment transport on hillslopes and implications for landscape morphology. Water Resources Research 35, 853–870.

Roering, J.J., Kirchner, J.W., Sklar, L.S., Dietrich, W.E., 2001a. Hillslope evolution by nonlinear, slope-dependent transport. Steady state morphology and equilibrium adjustment timescales. Journal of Geophysical Research-Solid Earth 106, 16499–16513.

Roering, J.J., Kirchner, J.W., Sklar, L.S., Dietrich, W.E., 2001b. Hillslope evolution by nonlinear creep and landsliding: an experimental study. Geology 29, 143–146.

Roering, J.J., Perron, J.T., Kirchner, J.W., 2007. Functional relationships between denudation and hillslope fonn and relief. Earth and Planetary Science Letters 264, 245–258.

Schumm, S.A., 1967. Rates of surficial rock creep on hillslopes in Western Colorado. Science 155, 560–562.

Selby, M.J., 1993. Hillslope materials and processes. Oxford University Press, Oxford, 451 pp.

Tucker, G.E., Bradley, D.N., 2010. Trouble with diffusion: reassessing hillslope erosion laws with a particle-based model. Journal of Geophysical Research 115, F00A10. doi:10.1029/2009JF001264.

Tucker, G.E., Slingerland, R.L., 1994. Erosional dynamics, flexural isostasy, and long-lived escarpments: a numerical modeling study. Journal of Geophysical Research, Solid Earth and Planets 99, 12,229–12,243.

Tyler, A., Carter, S., Davidson, D., Long, D., Tipping, R., 2001. The extent and significance of bioturbation on ^{137}Cs distributions in upland soils. Catena 43, 81–99.

Wallbrink, P.J., Murray, A.S., 1996. Distribution and variability of Be-7 in soils under different surface cover conditions and its potential for describing soil redistribution processes. Water Resources Research 32, 467–476.

Walling, D.E., He, Q., 1999a. Improved models for estimating soil erosion rates from cesium-137 measurements. Journal of Environmetal Quality 28, 611–622.

Walling, D.E., He, Q., 1999b. Using fallout lead-210 measurements to estimate soil erosion on cultivated land. Soil Science Society Of America Journal 63, 1404–1412.

Walther, S.C., Roering, J.J., Almond, P.C., Hughes, M.W., 2009. Long-term biogenic soil mixing and transport in a hilly, loess-mantled landscape: Blue Mountains of southeastern Washington. Catena 79, 170–178.

Whiting, P.J., Bonniwell, E.C., Matisoff, G., 2001. Depth and areal extent of sheet and rill erosion based on radionuclides in soils and suspended sediment. Geology 29, 1131–1134.
Willenbring, J.K., von Blackenburg, F., 2010. Meteoric cosmogenic Beryllium-10 adsorbed to river sediments and soil: applications for Earth-surface dynamics. Earth Science Reviews 98, 105–122.
You, C., Lee, T., Li, Y., 1989. The partition of Be between soil and water. Chemical Geology 77, 105–118.
Young, A., 1960. Soil movement by denudational processes on slopes. Nature 188, 120–122.
Young, A., 1963a. Soil movement on slopes. Nature 200, 129–130.
Young, A., 1963b. Some field observations of slope form and regolith, and their relation to slope development. Transactions of the Institute of British Geographers 32, 1–29.

Biographical Sketch

Arjun Heimsath is a geomorphologist whose main interests are in quantifying the rates and processes of erosion in hilly and mountainous landscapes. These rates and processes are coupled by examination of the feedbacks driven by tectonic, climatic, and anthropogenic forcing. He uses diverse geochemical tools coupled with field work in field areas worldwide.

Matthew Jungers is a geomorphologist specializing in the application of cosmogenic nuclide geochemistry for quantifying the rates of Earth surface processes as well as Quaternary geochronology and landscape evolution. He received his MS from the University of Vermont, and is currently a doctoral candidate at Arizona State University.